Broadband Receiver Technology for Atmospheric Humidity, Temperature and Precipitation Sounding

P. Kangaslahti, D. Pukala, T. Gaier, S. Brown
Jet Propulsion Laboratory
California Institute of Technology
4800 Oak Grove Drive
Pasadena, CA 91109 USA

***Abstract*- The measurement of atmospheric humidity, temperature and precipitation are highly important for weather forecasting, atmospheric science and calibration of primary measurements. Radiometer measurements in the vicinity of oxygen and water molecule absorption lines at millimeter wave frequencies provide this data. We have characterized a broadband amplifier that will increase the sensitivity of sounding and other instruments at these frequencies. The measured InP monolithic millimeter-wave integrated circuit (MMIC) amplifier had more than 18 dB of gain from 100 to 180 GHz and 15 dB of gain up to 220 GHz. In WR-05 waveguide package it had 3.7 dB noise figure and enabled us to design WR-05 waveguide receiver with 4.1 dB noise figure. The typical microwave sounding satellites use primarily the 60 GHz oxygen line for temperature sounding, however, there are several advantages to be gained from observations near the 118.75 GHz oxygen line. For fixed aperture dimensions, a diffraction-limited 118 GHz system will yield twice the spatial resolution of a similar 60 GHz system. Additionally the sensitivity to clouds and precipitation at 118 GHz is typically greater than at 60 GHz. This greater sensitivity to hydrometeors enables improved detection of regions of heavy cloud and precipitation relative to that available using 60 GHz frequency window or sounding channels. The frequency channels in the proximity of 183 GHz are used for atmospheric sounding of water vapor.**

I. INTRODUCTION

The atmospheric sciences and weather forecasting have received significant attention in recent years due to hurricanes and predicted global climate change. These fields of research require continuous measurements that are obtained from both airplanes and satellites. The repeat rate of the full synthesized image is strongly dependent on the sensitivity of the instrumentation for the measurements. For this purpose we have characterized a recently developed InP LNA MMIC over a broad frequency range [1]. Additionally, the InP LNA MMIC will enable highly sensitive instruments for several other applications. We measured more than 80 GHz of bandwidth from 100 to 180 GHz from these LNAs. Several amplifiers at 100 to 200 GHz frequency range were reported previously [2]-[4], however, their usable operating frequency range was limited to 10 to 20 %. We demonstrate 60 % of operating frequency range. This is the widest bandwidth low noise amplifier result at these frequencies to date. The noise figure of the MMIC LNA was at 3 dB range based on the waveguide package measurements [5].

II. MILLIMETER WAVE INSTRUMENTS

Low noise millimeter wave receivers are required for several measurements in Earth sciences. We have primarily focused on temperature, humidity and precipitation sounding and atmospheric delay correction for altimeters in our instrumentation.

A. Geostationary Microwave Sounder

A geostationary microwave sounder is recommended in the NASA decadal survey of Earth science missions. This Precipitation and All-weather Temperature and Humidity (PATH) sensor will have a primary mission of observing hurricanes and severe storms. The sensor would operate in two spectral bands: near 50 GHz, with 4-6 channels, for temperature sounding and near 183 GHz, with 4-5 channels, for water vapor sounding. That would give the same functionality and capabilities as provided with current and future LEO sounders, such as the AMSU instruments. Table I summarizes the data products that can be generated with such a sensor system – this list corresponds to baseline capabilities equivalent to products generated with existing LEO systems (except for temporal and spatial characteristics)[6].

TABLE I
GEOSTAR BASELINE CAPABILITIES [6]

Parameter	Horiz. (km)	Vertical (km)	Temporal (min)	Accuracy
Tb (50 GHz)	50	N/A	3 per ch	<1 K
Tb (183 GHz)	25	N/A	5 per ch	<1 K
Temperature	50	2	~ 10	2 K
Water vapor	25	3	~ 20	25%
Liquid water	25	4	~ 20	40%
TPW	25	N/A	~ 20	10%
LWC	25	N/A	~ 20	20%
SST	50	N/A	~ 10	2K
Stability index	50	N/A	~ 20	N/A

In addition, a number of experimental products are under development that will have particular applicability to hurricanes and severe storms. A selected list is shown in Table II. These observations and derived products will be generated continuously, day and night, with a temporal resolution of 10-20 minutes in the central focus area. The "experimental" products include parameters that can currently only be produced from precipitation radar systems: rain rates, atmospheric ice content, convective intensity and finally, analysis of microwave sounder data from recent hurricane field campaigns indicate that the radiative effects of scattering from ice in deep convective systems is similar to the backscatter observed by radar – although with a lower vertical resolution.

TABLE II
GEOSTAR BASELINE EXPERIMENTAL CAPABILITIES [6]

Parameter	Horiz. (km)	Vertical (km)	Temporal (min)	Accuracy
Rain rate	25	N/A	20	TBD
Convective intensity	25	N/A	20	TBD
IWC	25	N/A	20	TBD
Wind vector	25	2	30	TBD

B. Airborne Temperature, Precipitation and Humidity Microwave Sounder

The High Altitude MMIC Sounding Radiometer (HAMSR) is an atmospheric sounder which was designed and built at the Jet Propulsion Laboratory under a grant from the NASA Instrument Incubator Program in 2001 and uses the most advanced technology available to date to achieve excellent performance in a small package. HAMSR has 8 sounding channels near the 60 GHz oxygen line complex, 10 channels near the 118.75 GHz oxygen line and 7 channels near the 183.31 GHz water vapor line [7].

The typical microwave sounding satellites use primarily the 60 GHz oxygen line for temperature sounding, however, there are several advantages to be gained from observations near the 118.75 GHz oxygen line. For fixed aperture dimensions, a diffraction-limited 118 GHz system will yield twice the spatial resolution of a similar 60 GHz system. Additionally the sensitivity to clouds and precipitation at 118 GHz is typically greater than at 60 GHz. This greater sensitivity to hydrometeors enables improved detection of regions of heavy cloud and precipitation relative to that available using 60 GHz frequency window or sounding channels. This feature, along with the higher spatial resolution available from diffraction-limited 118 GHz systems permits relatively weak precipitation cells to be remotely probed, particularly those over land [8]. For snowfall, the sounding channels produce 60% of all retrievals with errors below 100% for rates smaller than 1 mm h^{-1}, and 50%-80% of the cases have errors below 50% for more intense snowfall. [9]. A table of the HAMSR frequencies and measured NEΔTs at ambient are shown in Table III [7].

TABLE III
HAMSR CHANNEL CHARACTERISTICS [7]

Chan #	Center freq. [GHz]	Offset [GHz]	Wt-func. Peak [mb or mm]	NEΔT [K]
I-1	118.75	-5.500	Sfc/[30 mm]	0.62
I-2	"	-3.500	Surface	0.46
I-3	"	-2.550	Surface	0.68
I-4	"	-2.050	1000 mb	0.92
I-5	"	-1.600	750 mb	1.2
I-6	"	-1.200	400 mb	0.83
I-7	"	±0.800	250 mb	0.48
I-8	"	±0.450	150 mb	0.51
I-9	"	±0.235	80 mb	0.60
I-10	"	±0.120	40 mb	0.67
II-1	50.30	0	**Sfc/[100 mm]**	0.40
II-2	51.76	0	Surface	0.27
II-3	52.80	0	**1000 mb**	0.21
II-4	53.596	±0.115	**750 mb**	0.18
II-5	54.40	0	**400 mb**	0.17
II-6	54.94	0	**250 mb**	0.16
II-7	55.50	0	**150 mb**	0.17
II-8	56.02 & 56.67	0	90 mb	0.18
III-1	183.31	-17.0	[11 mm]	0.61
III-2	"	±10.0	[6.8 mm]	0.94
III-3	"	±7.0	**[4.2 mm]**	0.98
III-4	"	±4.5	[2.4 mm]	1.0
III-5	"	±3.0	**[1.2 mm]**	1.3
III-6	"	±1.8	[0.6 mm]	1.0
III-7	"	±1.0	**[0.3 mm]**	1.5

The HAMSR brightness temperature measurements can be used to indicate the convective intensity of a storm, provide precipitation estimates and information on ice microphysics [7]. Five pairs of 60 and 118 GHz channels have nearly matched clear air weighting functions. In clear air, the difference between these channels will be nearly zero, but in the presence of deep convection, the brightness temperature scattering depression due to the ice particle content of the cloud will be much greater at 118 GHz than at 60 GHz. Because the clear air weighting function peaks are distributed vertically through the atmosphere, observing the difference between the matched channels gives an indication of both the intensity and height of the precipitation [7]. The approximate heights in the atmosphere where each difference will be sensitive to precipitation are shown in Fig. 1. For example, the difference between channels I-7 and II-6 give an indication of ice content above about 14 km and the next lower channel pair provides information on the precipitation content above about 11 km.

HAMSR observed Hurricane Emily from the ER-2 on July 17, 2005 [7]. HAMSR "cloud slices" reveal intense convection in the eyewall region, with storm tops reaching above 15 km on North-West side of the eyewall. Two transits across the eye wall are shown in Fig. 2., the first in a N-W heading and the second in a N-E heading. The five HAMSR cloud slicing levels are shown with the nadir ER-2 Doppler Radar (EDOP) X-band reflectivity profile in the background. It is evident that HAMSR is able to assess the three-dimensional structure of the storm [7].

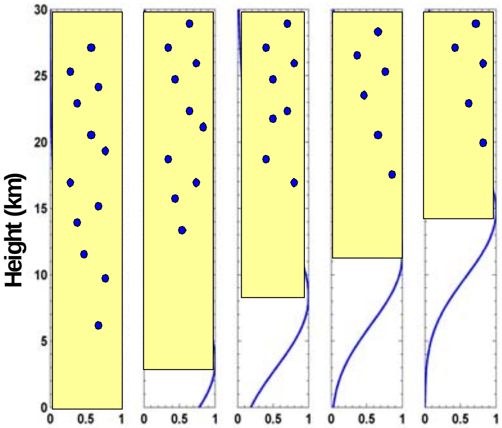

Fig. 1. Approximate HAMSR "Cloud Slicing" altitudes [7].

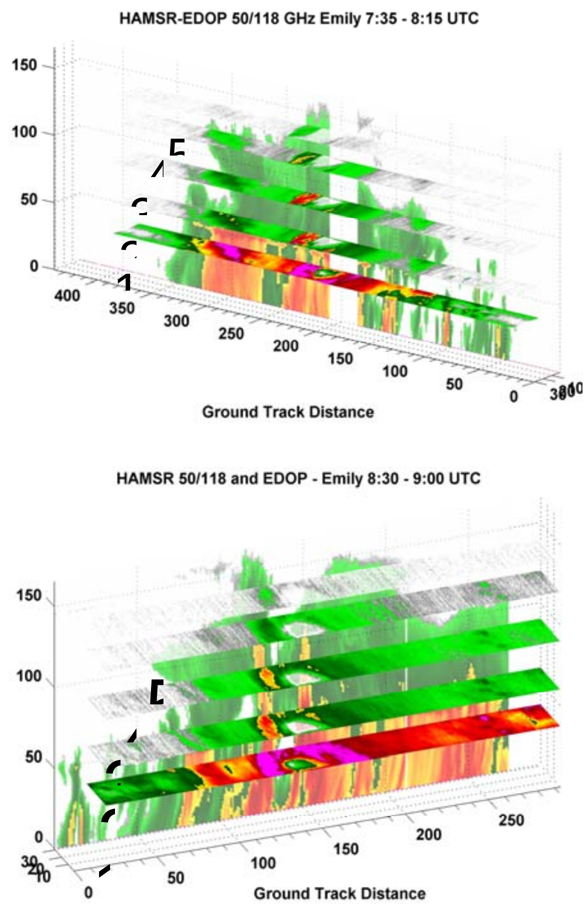

Fig. 2. HAMSR "cloud slices" from Hurricane Emily [7].

C. Wet Tropospheric Correction for Path Delay in Altimetry

Radar altimetry missions require calibration of the atmospheric properties to correct for variations in the radar signal path delay (PD) and these corrections become more difficult as the satellite approaches the coast (Fig. 3). Ship based and airborne measurements show significant short scale water vapor variability in coastal areas. Variations did not necessarily correlate with distance to land. Furthermore, land contamination will cause errors in the path delay calibration. It can be divided into three categories [10]: 1) Far sidelobe contamination (> 75 km from coast) that is correctable to acceptable levels (~ 1mm), 2) near sidelobe contamination (25 – 75 km from coast) that is more difficult to correct, however, it is possible (~2-4 mm) and 3) main beam contamination (0 – 25 km from coast) that is very difficult to correct (20-40 mm). By adding high frequency channels to current instruments the PD estimates in coastal regions can be improved [10].

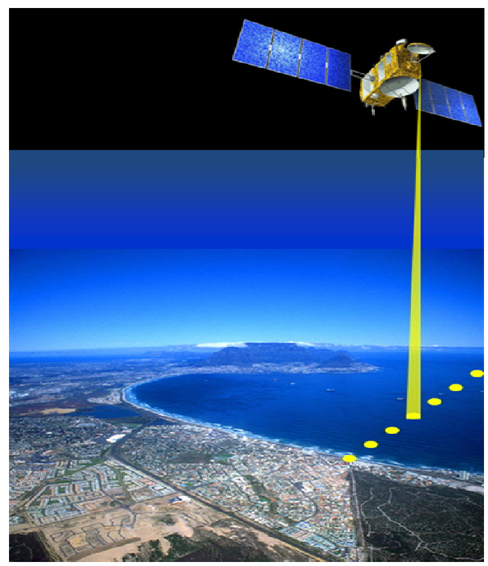

Fig. 3. Coastal altimetry from satellite [10].

Preliminary feasibility study investigated the addition of 92, 130 and 166 GHz channels to traditional 18-37 GHz design [10]. High frequency channels are used to estimate water vapor when traditional low-frequency channels become contaminated by land. Simulated PD retrieval performance is better than 1 cm at distances of 3 km from land. In the simulations errors were binned by standard deviation of PD and cloud liquid water (CLW) on coastal approach. Different permutations of channel combinations were used to verify that errors generally < 1 cm for 3 frequency retrieval [10]. Errors increase as variability of both CLW and PD increase [10]. These results are demonstrated in Fig. 4.

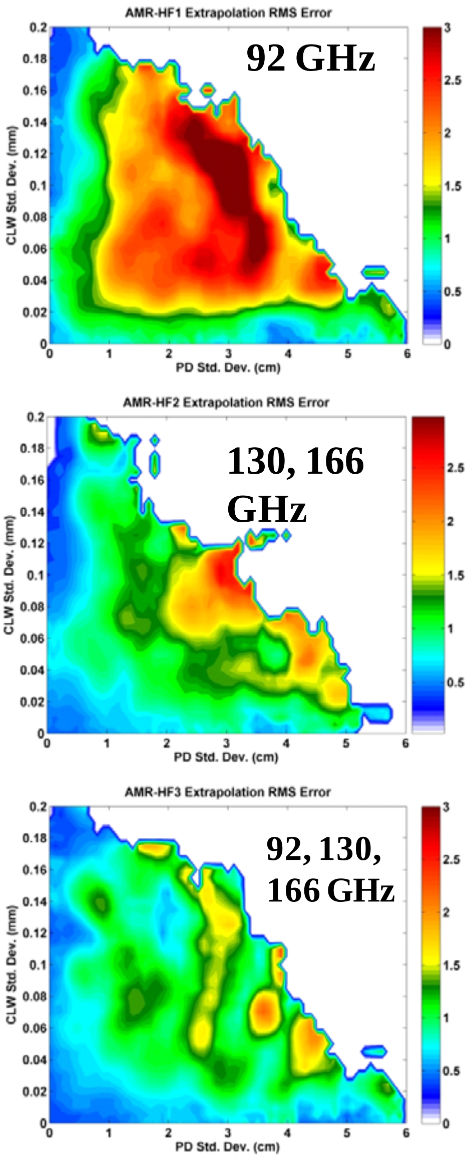

Fig. 4. Simulated PD retrieval performance with different observation frequency combinations [10].

III. LNA TECHNOLOGY

The LNA technology for the 100 to 180 GHz frequency range is based on devices with sufficiently high gain at the targeted operating frequency. The 35 nm InP device technology provides sufficiently high transconductance per device area [11]. The LNAs were developed based on this device technology with microstrip transmission lines on 2 mil thick substrate [11]. The design incorporated two-finger HEMT devices having gate widths of 15 µm each, for a total gate periphery of 30 µm for each transistor stage. The amplifier demonstrated over 18 dB of gain from 100 GHz to 180 GHz as is shown in Fig. 5. Furthermore, there is gain beyond 220 GHz at higher than 15 dB level. This measurement is composed of the WR-10 (75 to 110 GHz), WR-08 (90 to 140 GHz) and WR-05 (140 to 220 GHz) test results [1].

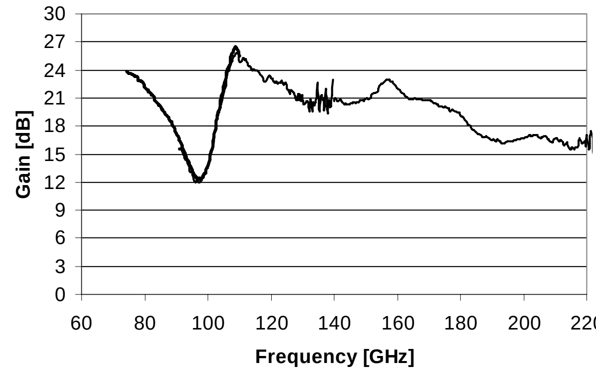

Fig. 5. The measured gain of the broadband MMIC LNA at 75 to 220 GHz frequency range [1].

Fig. 6 shows the measurement test set-up with the LNA under measurement. In order to suppress low-frequency (< 1 GHz) gain and potential oscillations which are commonly observed with very high frequency transistors, we had GGB industries mount bypass capacitors right at the tips of the gate DC needles. The first device in the LNA has a separate gate control and the second and third stage devices gates are connected together on the chip. The drains of all three devices are connected together, so for the drain biasing we used a single coaxial probe that has inherently low impedance (50 Ohm).

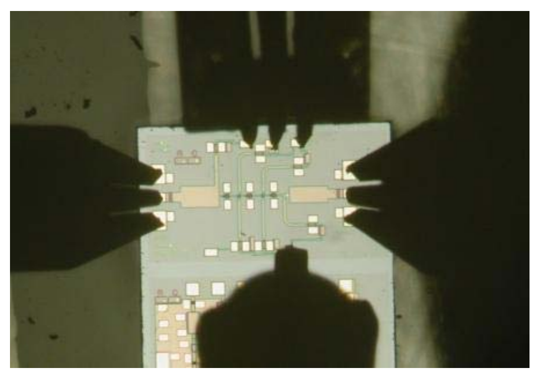

Fig. 6. Photograph of the measurement of the broadband MMIC LNA [1].

The microstrip LNA noise temperature results are shown in Fig. 7 [5]. These results demonstrate a measured noise temperature of 370 K at 160 GHz, which is half of the previous state-of-the-art. The graph shows noise temperature and noise figure results from 155 to 190 GHz in addition to the calculated gain [5]. The ripple in the gain pattern is caused by the extra transmission lines and wirebonds at the output side of the LNA in the housing. With an optimized packaging we expect the gain to have significantly less ripple.

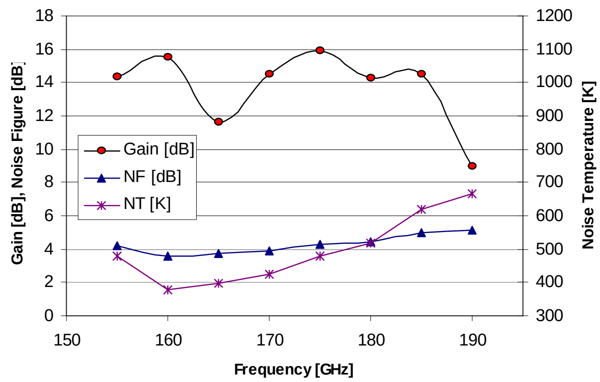

Fig. 7. Measured results for the waveguide MMIC LNA. The noise temperature (NT) of this LNA is < 400 K, less than half of the previous state-of-the-art. The noise figure of the LNA is NF = 3.7 dB [5].

The noise temperature of the LNA increases towards the 180 GHz frequency due to the mismatch caused by the wirebond from the input waveguide probe to the LNA. A tuning element before the wirebond should minimize this effect and improve the noise temperature at 180 GHz. The input waveguide and waveguide to microstrip transition has a simulated loss of L=0.8 dB. Thus, the noise figure of the LNA MMIC is expected to be roughly NF=3dB [5]. In space application this LNA would be operated at lower physical temperature than ambient, so we tested the noise temperature of the LNA at different operating temperatures. Fig. 8. shows the noise temperature of the LNA vs. physical temperature [5]. This testing was done in cryogenic chamber, so we were able to test down to 30 K physical temperature. The expected operating temperature of the GeoSTAR receivers will be T_{phys}=240 K. At this temperature the the noise temperature of the LNA is below the required T_n=400 K. The LNA has less than 100 K noise temperature at cryogenic temperatures (T_{phys} = 30K) [5].

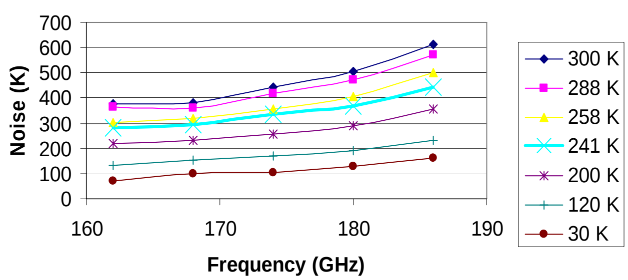

Fig. 8. Measured gain and noise of the double sideband receiver. A single sideband receiver will have same noise temperature [5].

Finally, we cascaded the two waveguide MMIC LNAs with a low LO power VDI diode mixer. Fig. 9 shows the measured results for this double sideband second harmonic receiver. The receiver has 15 dB of conversion gain from 165 to 183 GHz and noise temperature of 430 to 470 K over the same frequency band [5]. This receiver operated with low DC bias power (55 mW) and required only .1 mW of LO power at W-band. These low DC and LO power results are promising for the implementation of large arrays, where power consumption of the receivers and LO distribution network are critical.

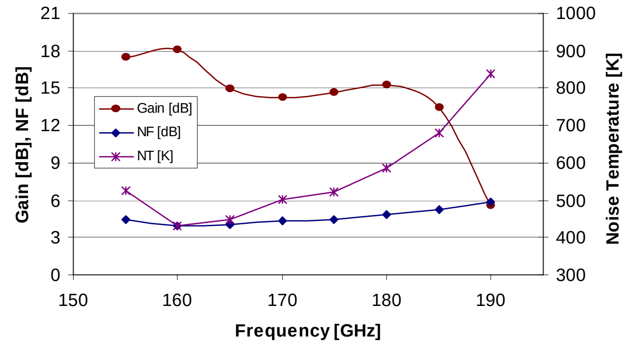

Fig. 9. Measured gain and noise of the double sideband receiver. A single sideband receiver will have same noise temperature [9].

IV. Conclusions

We have demonstrated the on-wafer characterization of a broadband millimeter wave InP MMIC LNA. Continuous low noise amplification was shown from 100 GHz to 180 GHz. The amplifier had more than 10 dB gain over the whole measurement range from 75 to 220 GHz. Furthermore we demonstrated a factor of two reduction in noise temperature of MMIC LNAs at 180 GHz frequency band. This result was enabled by the significant improvement in InP MMIC process achieved within the last years.

Applications of this work include low noise receivers for atmospheric sounding of humidity, temperature and precipitation. The MMIC LNA operates with low DC power and has high gain to enable us to design low noise and low power receivers for large arrays, such as the GeoSTAR synthetic thinned aperture radiometer instrument.

Acknowledgment

This work was supported by the by the NASA ESTO Advanced Component Technologies ACT-05 program. This research was carried out at the Jet Propulsion Laboratory, California Institute of Technology, and was sponsored by National Aeronautics and Space Administration.

References

[1] P. Kangaslahti, W. R. Deal, X.B. Mei and R. Lai, "Broadband Characterization of a 100 to 180 GHz Amplifier" *Proc. IEEE Aerospace Conference,* March 1-8, 2008, Big Sky, MT

[2] D. Dawson, L. Samoska, A.K. Fung, K. Lee, R. Lai, R. Grundbacher, P.H. Liu, R. Raja, "Beyond G-band: a 235 GHz InP MMIC amplifier," *IEEE Microwave and Components Letters*, Volume 15, Issue 12, Dec. 2005, pp. 874 – 876.

[3] A. Tessmann, "220-GHz metamorphic HEMT Amplifier MMICs for High-Resolution Imaging Applications," in *IEEE Journal of Solid-State Circuits*, Volume 40, Issue 10, Oct. 2005, pp. 2070 – 2076.

[4] S. Weinreb, T. Gaier, R. Lai, M. Barsky, Y.C. Leong and L. Samoska, "High-Gain 150-215-GHz MMIC Amplifier with Integral Waveguide Transitions" *IEEE Microwave Theory and Techniques Components Letters*, Volume 9, Issue 7, July 1999, pp. 282 – 284

[5] P. Kangaslahti, D. Pukala, T. Gaier, W. R. Deal, X.B. Mei and R. Lai, "Low Noise Amplifier for 180 GHz Frequency Band" *Proc. IEEE International Microwave Conference,* June 14-18, 2008, Atlanta, GA.

[6] B. Lambrigtsen, A. Tanner, T. Gaier, P. Kangaslahti and S. Brown, "Prototyping GeoSTAR for the PATH Mission" *Proceedings NASA Science Technology Conference*, June 19-21, 2007, University of Maryland University College, Adelphi, MD

[7] S. Brown, B. Lambrigtsen, A. Tanner, J. Oswald, D. Dawson, R. Denning. "Observations of tropical cyclones with a 60, 118 and 183 GHz microwave sounder" *Proc. IEEE Geoscience and Remote Sensing Symposium*, July 2007, pp. 3317 – 3320.

[8] A. J. Gasiewski, J.W. Barrett, P.G. Bonanni and D.H. Staehlin, "Aircraft-based Radiometer Imaging of Tropospheric Temperature and Precipitation Using the 118.75-GHz Oxygen Resonance" *Journal of Applied Meteorology*, Volume 29, July 1990, pp. 620 – 632.

[9] P. Bauer, E. Moreau and S. Di Michele, "Hydrometeor Retrieval Accuracy Using Microwave Window and Sounding Channel Observations" *Journal of Applied Meteorology*, Volume 44, July 2005, pp. 1016 – 1032.

[10] S. Brown and B. Khayatian, "Wet Tropospheric Correction in Coastal Regions" *Coastal Detection Workshop,* Silver Spring, MD, Feb. 2008.

[11] X.B. Mei, W. Yoshida et. al. "35nm InP HEMT for Millimeter and Sub-Millimeter Wave Applications" *Proc. IEEE Indium Phosphide & Related Materials Conference*, May 2007. pp. 59 – 62.